

Limit and Shakedown Analysis for Plastic Design

M. Staat, M. Heitzer

Institute for Safety Research and Reactor Technology,
Forschungszentrum Jülich GmbH, D-52425 Jülich, Germany

Abstract

Limit and shakedown theorems are exact theories of classical plasticity for the direct computation of safety factors or of the load carrying capacity under constant and varying loads. Simple versions of limit and shakedown analysis are the basis of all design codes for pressure vessels and pipings. Using Finite Element Methods more realistic modeling can be used for a more rational design. The methods can be extended to yield optimum plastic design. In this paper we present a first implementation in FE of limit and shakedown analyses for perfectly plastic material. Limit and shakedown analyses are done of a pipe-junction and a interaction diagram is calculated. The results are in good correspondence with the analytic solution we give in the appendix.

1 NOMENCLATURE

b	body force	W_p	max. plastic dissipation
n	outer normal vector	$\beta, \beta_{limit}, \beta_{SD}$	load, limit and shakedown factor
p	surface traction	ϵ	actual strain
P_0, T_0	reference load	ϵ^E	elastic strain
w_p	density of plast. dissipation	$\epsilon^P, \dot{\epsilon}^P$	plastic strain and rate
t	time	ϵ^T	thermal strain
x	coordinate vector	μ, μ_1, μ_2	parameters
C_i	element compatibility matrix	$\rho, \dot{\rho}$	residual stress and rate
D, d, s, s_p, s_j	dimensions of the pipe-junction	ρ_i	dicrete eigen-stress vector
E	elasticity tensor	$\bar{\rho}$	time-independent residual stress
NG	number of Gaussian points	σ	actual stress
NV	number of load vertices	σ_0	yield stress
$P, P_{el}, P_{elastic}$	actual and elastic pressure	σ^E	fictitious elastic stress
$P(t), P_{limit}$	load and limit pressure	σ_i^E	discrete fict. elast. stress vector
P_a, \dots, P_g	actual stresses	Φ	yield function
T, T_{el}	actual and elastic temperature	$\Omega, \partial\Omega$	structure and its boundary
T_i, T_a	inner and outer temperature	\mathcal{L}	load domain

1 Introduction

Passive components in power plants are designed on a structural mechanics basis for internal pressure, additional mechanical loading, and thermal loading. Mechanical and thermal stress respectively decrease and increase with wall-thickness. The elastic range is bounded by allowable stress. If design is based on elastic stress assessment, the minimum total stress $\sigma = \sigma_{mech} + \sigma_{therm}$ may define the optimum wall-thickness of a heat exchanger tube for given heat flow density.

The elastic strain range is rather small. It is impossible to design a structure with considerable thermal loading within the elastic range. Thermo-shock or other residual stresses may push stress further into the plastic range locally. Therefore plastic analysis is used in design of passive components made of ductile material. Plastic design cannot be based on stress assessment, because there is no stress to bound the plastic range from failure domains. Instead plastic design has to consider the characteristic development of plastic strains towards structural failure [?]:

- Instantaneous collapse by unrestricted plastic flow at limit load.
- Incremental collapse by accumulation of plastic deformations over subsequent load cycles (ratchetting).
- Low Cycle Fatigue (LCF) by alternating plasticity.
- Plastic instability of slender compression members (limit analysis does not apply for this failure mode).

The above optimum wall-thickness may not be a rational choice for inelasticity. Plastic failure modes cannot be assessed from the state of stress, because different stresses interact in a nonlinear way towards structural failure. Design codes try to maintain the stress assessment by introducing e.g. the concept of primary and secondary stress. Secondary stress is defined to have no influence on the limit load. There is little guidance for the designer how to recognize secondary stress. However, it is known from limit analysis that thermal stress and all other residual stresses are secondary stresses, provided they do not significantly alter the geometry of the structure or the yield surface of its material [?] (for experimental evidence see [?]).

In principle the possible structural failure may be reproduced in a detailed incremental plastic analysis if it can be continued towards the limits. Generally this is prohibitively expensive in the design stage and the necessary details of load history or of the constitutive equations may not be available. If computation is stopped away from the limit, any prediction of failure is based on extrapolation. In particular the elastically computed stress may be of little use in limit load prediction, because limit load is independent of the elastic constants (Young's modulus, Poisson ratio) [?].

To avoid the above short-comings "Limit- and shakedown load form - in this or another way - the basis of the design concept of modern design codes such as ASME-Code, Section VIII-Division 2, British Standard 5500, ISO-DIS 2694 and the AD-Merkblätter." ([?], translated from the German). Load is the most modern word in this quotation. Component geometry, dimensions and design operation are determined by the allowable load. This design load may not be simply derived from the detailed knowledge of stress and strain history. The interpretation of stress and stress components is not self-evident [?]. The direct computation of the load carrying capacity is the objective of limit- and shakedown analyses (not applicable for the stability problem). They are used for design in the form of rules to derive allowable stress intensities [?], limit load formulae [?], and interaction diagrams (like Bree and Brussels diagrams, [?]). This current design practice rests on simplifying assumptions for geometry, loading and constitutive equation.

We will show in this contribution how these assumptions may be avoided by using the Finite Element Method (FEM) for limit- and shakedown analysis. Some twenty years ago the Pressure Vessel and Piping Division of ASME has invited researchers to develop software for design by limit analysis using the FEM [?]. But until recently this approach was limited to relatively small Finite-Element-Models [?]. We have implemented limit and shakedown analysis into the general purpose FEM program PERMAS employing a subspace technique which can handle large models. FEM based limit and shakedown analyses may be used to compute interaction diagrams for any complex component under two-parameter loading. These may be used to decide on allowable loading ranges for the structure. More complex loading may be analysed. But they cannot be represented in a similarly visual manner. The analyses may be performed at computing times and costs of only 2-10 standard elastic FEM analyses. Thus design variants may be compared and an optimum choice be made [?]. The present FEM implementation of this ongoing research is restricted to ideal plasticity with constant material coefficient. The extension to hardening material will be one of the next steps.

Limit and shakedown analysis may be extended towards optimum plastic design. This option was e.g. realized by the program CEPAO (Calcul Elasto-Plastique, Analyse-Optimisation) for plane frame structures [?]. The optimum cross sections of the beams in the structure are obtained and checked for buckling of compression members. A development towards optimum plastic design could be a follower of the present project. From the computational burden it is clear that the highly effective limit and shakedown analysis will be the only possible approach for a long time [?].

Limit and shakedown theorems provide rules and guidance for design. It is e.g. easily shown that adding of weightless material may not decrease the limit load [?]. In the appendix we prove, that for a structure made of linear kinematic hardening material which fails locally under proportional loading (e. g. pressure and temperature), the shakedown range is obtained by expansion of the elastic range by a factor of 2. This simple result is independent of the hardening exponent and holds also for perfect plastic material. Therefore the kinematic hardening effect bears no profit for such structures (e. g. pipe-junction, plate with a hole, see [?]).

2 Theorems of limit load and elastic shakedown

Although being simplifying methods limit and shakedown analyses are exact theories of plasticity, which do not contain any restrictions or assumptions other than sufficient ductility of the material. Simplicity is achieved with respect to the required input data and to reduced computational effort. This is reached by restricting analysis to the direct computation of the safety factor.

Static theorems are formulated in terms of stress and define safe structural states giving an optimization problem for safe loads. The maximum safe load is respectively, the limit load avoiding collapse and the (elastic) shakedown load avoiding ratchetting and LCF. Alternatively, kinematic theorems are formulated in terms of kinematic quantities and define unsafe structural states yielding a dual optimization problem for the minimum

of limit or shakedown loads. Any admissible solution to the static or kinematic theorem is a true lower or upper bound to the safe load, respectively. Both can be made as close as desired to the exact solution. If lower and upper bound coincide the exact solution is found. To obtain conservative solutions the static approach is used, which is also numerically more convenient.

Static limit load theorem:

An elastic–plastic structure will not collapse under monotone loads if it is in static equilibrium and if the yield function is nowhere violated. The limit load is the maximum safe load.

Static shakedown theorem:

An elastic–plastic structure will not fail with macroscopic plasticity under time variant loads if it is in static equilibrium, if the yield function is nowhere and at no instance violated, and if all plastic deformations fade away, i.e. if $\lim_{t \rightarrow \infty} \dot{\boldsymbol{\varepsilon}}^P(t) = \mathbf{0}$. The shakedown load is the maximum safe load.

If observation starts after few cycles, there may be no difference between pure elastic behaviour and shakedown, because in elastic shakedown the material becomes eventually elastic. A difference can only be made if the plastic part of the load history is known.

To make them operational we will now formalize the static theorems. The given structure Ω is assumed to be composed of material points denoted by their coordinate vectors $\mathbf{x} \in \Omega$. In the geometrically linear theory an additive decomposition in elastic, plastic and temperature strains of the strains $\boldsymbol{\varepsilon}$ is possible.

$$\boldsymbol{\varepsilon} = \boldsymbol{\varepsilon}^E + \boldsymbol{\varepsilon}^P + \boldsymbol{\varepsilon}^T. \quad (1)$$

The elastic strains $\boldsymbol{\varepsilon}^E = \mathbf{E}^{-1} : \boldsymbol{\sigma}$ are obtained from the inverse of the fourth–order elasticity tensor \mathbf{E} by Hooke’s law. For an elastic, perfectly plastic material plastic strains $\boldsymbol{\varepsilon}^P$ occur if a yield function f reaches the yield stress σ_0 (and a loading condition is satisfied). The von Mises yield function is chosen. This function is preferred because it is continuous differentiable. But most theorems of plasticity theory hold also for Tresca yield function. Material stability in the sense of Drucker’s postulate is assumed. Thus the yield surface bounded by $\Phi = \sigma_0^2$ is convex.

For a load increasing with load factor β the above necessary conditions for a safe state of Ω with traction boundary $\partial\Omega_\sigma$ (with outer normal \mathbf{n}) and yield function Φ under body forces $\beta\mathbf{b}$ and surface loads $\beta\mathbf{p}$ read

$$\Phi(\boldsymbol{\sigma}) \leq \sigma_0^2 \quad \text{in } \Omega \quad (2)$$

$$\text{div } \boldsymbol{\sigma} = \beta\mathbf{b} \quad \text{in } \Omega \quad (3)$$

$$\boldsymbol{\sigma} \mathbf{n} = \beta\mathbf{p} \quad \text{on } \partial\Omega_\sigma. \quad (4)$$

The limit load factor $\beta_{limit} = \max \beta$ is a safety factor. This leads to the mathematical optimization problem formulated in static quantities (stress $\boldsymbol{\sigma}$)

$$\max \quad \beta \quad (5)$$

$$\text{such that (s. t.)} \quad \text{restrictions (2) – (4) hold.} \quad (6)$$

The concepts for time-variant loading are more involved. Time is denoted by t . The stresses $\boldsymbol{\sigma}$ can be decomposed into fictitious elastic stresses $\boldsymbol{\sigma}^E$ and residual stresses $\boldsymbol{\rho}$ by

$$\boldsymbol{\sigma} = \boldsymbol{\sigma}^E + \boldsymbol{\rho}. \quad (7)$$

$\boldsymbol{\sigma}^E = \mathbf{E} : \boldsymbol{\varepsilon}$ are stresses which would appear in an infinitely elastic material, so that the $\boldsymbol{\rho}$ result from plastic deformations.

The residual stresses (eigen stresses) $\boldsymbol{\rho}$ satisfy the homogeneous static equilibrium and boundary conditions

$$\operatorname{div} \boldsymbol{\rho} = \mathbf{0} \quad \text{in } \Omega \quad (8)$$

$$\boldsymbol{\rho} \mathbf{n} = \mathbf{0} \quad \text{on } \partial\Omega_\sigma. \quad (9)$$

One criterion for an elastic, perfectly plastic material to *shake down elastically* is that the plastic strains $\boldsymbol{\varepsilon}^P$ and therefore the residual stresses $\boldsymbol{\rho}$ become stationary for given loads $\mathbf{P}(t) = (\mathbf{b}, \mathbf{p})$ in a load domain \mathcal{L} :

$$\begin{aligned} \lim_{t \rightarrow \infty} \dot{\boldsymbol{\varepsilon}}^P(\mathbf{x}, t) &= \mathbf{0}, \\ \lim_{t \rightarrow \infty} \dot{\boldsymbol{\rho}}(\mathbf{x}, t) &= \mathbf{0}, \quad \forall \mathbf{x} \in \Omega. \end{aligned} \quad (10)$$

In every considered failure mode exist points \mathbf{x} of the structure where condition (10) is violated. Thus there exists at least one point \mathbf{x} for which the density of the plastic energy dissipation w_p per unit volume

$$w_p(\mathbf{x}, t) = \int_0^t \boldsymbol{\sigma}(\mathbf{x}, \tau) \dot{\boldsymbol{\varepsilon}}^P(\mathbf{x}, \tau) d\tau \quad (11)$$

increases indefinitely in time. To avoid the possibility of plastic failure the maximum possible plastic energy dissipation

$$W_p(\mathbf{x}) = \lim_{t \rightarrow \infty} w_p(\mathbf{x}, t) \leq c(\mathbf{x}) \quad (12)$$

must be bounded above for all points $\mathbf{x} \in \Omega$. We restrict ourselves to the shakedown criterion (10). This means, that independent of the loading history the system has to approach asymptotically an elastic limit state. For details of the extended theorem see [?]. The following static shakedown theorem holds [?], [?]:

Theorem (Melan):

If there exists a factor $\beta > 1$ and a time-independent residual stress field $\bar{\boldsymbol{\rho}}(\mathbf{x})$ with $\int_\Omega \bar{\boldsymbol{\rho}} : \mathbf{E} : \bar{\boldsymbol{\rho}} d\Omega < \infty$, such that for all loads $\mathbf{P}(t) \in \mathcal{L}$

$$\Phi[\beta \boldsymbol{\sigma}^E(\mathbf{x}, t) + \bar{\boldsymbol{\rho}}(\mathbf{x})] \leq \sigma_0^2 \quad \forall \mathbf{x} \in \Omega \quad (13)$$

is satisfied, then the structure will shake down elastically under the given load domain \mathcal{L} .

The greatest value β_{SD} which satisfies the theorem is called *shakedown-factor*. The static shakedown theorem is formulated in terms of stresses and gives a lower bound to β_{SD} . A dual formulation in the sense of mathematical optimization is given by Koiter's kinematic theorem [?], which is formulated in terms of kinematic quantities and yields an upper bound of β_{SD} . The objective of limit and shakedown analyses is to find bounds to the limit- and shakedown-factors β_{limit} and β_{SD} . This leads to the mathematical optimization problem

$$\max \quad \beta \quad (14)$$

$$\text{s. t.} \quad \Phi[\beta \boldsymbol{\sigma}^E(\mathbf{x}, t) + \bar{\boldsymbol{\rho}}(\mathbf{x})] \leq \sigma_0^2 \quad \forall \mathbf{x} \in \Omega \quad (15)$$

$$\text{div } \bar{\boldsymbol{\rho}}(\mathbf{x}) = \mathbf{0} \quad \forall \mathbf{x} \in \Omega \quad (16)$$

$$\bar{\boldsymbol{\rho}}(\mathbf{x}) \mathbf{n} = \mathbf{0} \quad \forall \mathbf{x} \in \partial\Omega_\sigma \quad (17)$$

with infinitely many restrictions, which is reduced to a finite problem by FEM discretization. Shakedown analysis gives the largest range in which the loads may safely vary with arbitrary load history. If the load domain \mathcal{L} shrinks to the point of monotone load, limit analysis is obtained as special case.

In the case of a temperature-dependent yield function $\Phi(T)$ the shakedown theorem of MELAN should be modified (see [?], [?]).

3 Discretization and optimization

The structure is divided into N finite elements with NG Gaussian points i . The general purpose FEM program PERMAS [?] was chosen to implement Melan's theorem, because it is sufficiently open to the user allowing to implement limit and shakedown analysis, which means a radical departure from current FEM concepts and solution steps, without any need of support by the PERMAS developers. PERMAS calculates the load dependent elastic stress vectors $\boldsymbol{\sigma}_i^E(t)$ by means of a displacement method [?]. The discretized homogeneous equilibrium conditions of the residual stresses can be noted as (see [?], [?])

$$\sum_{i=1}^{NG} \mathbf{C}_i \boldsymbol{\rho}_i = \mathbf{0}, \quad (18)$$

where the \mathbf{C}_i are respectively the element compatibility matrices and the discrete eigen-stress vector. This equation represents a discretized formulation of equations (16) and (17). In convex load domains \mathcal{L} in the form of a polyhedron every load $\mathbf{P}(t)$ can be represented as a convex combination

$$\mathbf{P}(t) = \sum_{j=1}^{NV} \mu_j \mathbf{P}(j) \quad \text{with } 0 \leq \mu_j \quad \text{and} \quad \sum_{j=1}^{NV} \mu_j = 1 \quad (19)$$

of the NV vertices $\mathbf{P}(j)$ of the polyhedron. From convex optimization theory (see [?]) follows, that inequality (15) only has to be satisfied at the vertices of \mathcal{L} . So the condition

(15) should be transformed with the stresses $\sigma_i^E(j)$ as fictitious elastic response to vertex $\mathbf{P}(j)$ at the Gaussian point i into

$$\Phi[\beta\sigma_i^E(j) + \bar{\rho}_i] \leq \sigma_0^2 \quad i = 1, \dots, NG, \quad j = 1, \dots, NV. \quad (20)$$

The $N + 1$ unknowns of the problem are β and the residual stresses $\bar{\rho}_i$. So this is a large scale optimization problem for a realistic Finite-Element-Model. Using a basis-reduction method (see [?]) the number of unknowns can be reduced in a subspace so that the final convex optimization problem has only a few unknowns (say 4,...,7). The reduced problem is convex, because the restrictions and the objective function are convex. Thus every local minimum is a global minimum (see [?]) and a solution of the problem is unique. Instead of infinitely many restrictions and unknowns in the continuous case, after the complete discretization there are only $NG \times NV$ restrictions and $d + 1$ unknowns. Starting from unpublished work of Prager this subspace technique was developed in [?] and extended in [?] (for details see also [?]). In every reduction step the problem is solved by a self-implemented SQP-method (Sequential Quadratic Programming) with augmented Lagrangian type line search function (see [?], [?]). Armijo's step length rule and BFGS matrix update are used. However, numerical tests show that the algorithm may become even faster without any update. Because of the small numbers of unknowns and the large number of restrictions, the quadratic sub-problems are solved by an active-set-strategy (see [?]). Derivatives are calculated analytically avoiding automatic differentiation methods.

In every sequential step k a direction is generated for which an improved load factor β^k is calculated. If the new direction is small enough, the first convergence criterion is fulfilled and another equilibrium iteration is started. After the sequential step there is an improvement of the load factor. If the relative improvement $(\beta^k - \beta^{k-1})/\beta^{k-1}$ is smaller than a given constant, the second convergence criterion is fulfilled and the algorithm stops. For a flowchart of the limit and shakedown analysis see Fig. 1.

4 Pipe-Junction

The pipe-junction is subjected to internal pressure P and a variable inner temperature T_i . The temperature T_e on the external surface of the pipe-junction is equal to the ambient temperature assumed to be zero for all times. For $T_i = T_e$ and $p = 0$ the system is assumed to be stress-free. The material data (Young's modulus, Poisson ratio and yield stress) are chosen to be temperature independent.

The pipe-junction is discretized with 125 solid 27-node hexahedron elements (HEXEC27). The discrete stresses were calculated in the 8 vertices of the elements so there are 1000 stresses in limit and 2000 – 4000 stresses in shakedown analysis. The FE-mesh and the essential dimensions of the pipe-junction are represented in Fig. 2. All computations were performed on the same workstation DEC 3000 Model 800 AXP using version IV of PERMAS [?].

The following loading conditions are investigated.

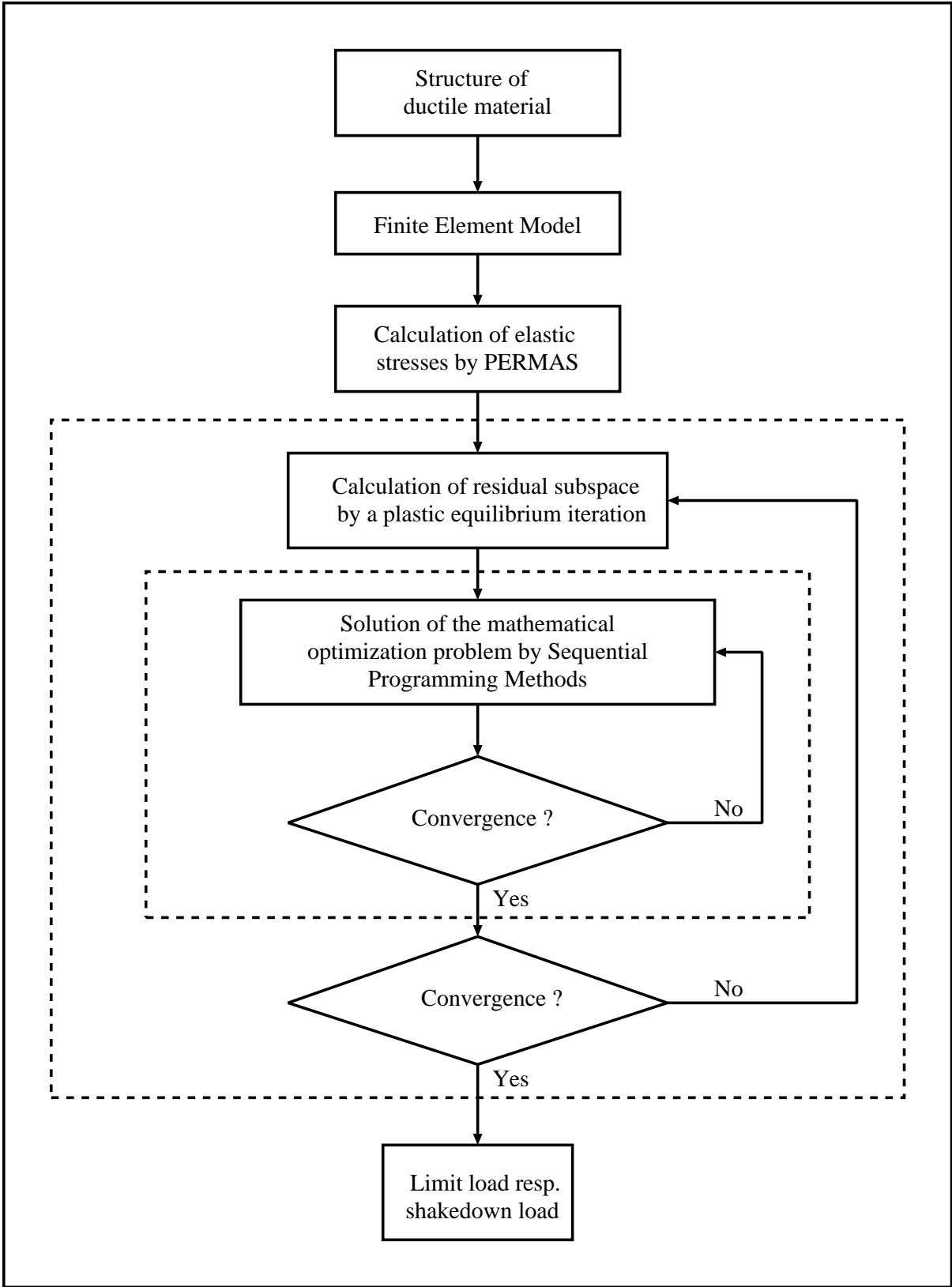


Figure 1: Flowchart of limit and shakedown analyses

1. Pressure P and temperature T_i vary simultaneously with $\frac{P}{T} = \text{const.}$ (one-parameter loading):

$$\begin{aligned} 0 &\leq P \leq \beta\mu P_0, \\ 0 &\leq T_i \leq \beta\mu T_0, \quad 0 \leq \mu \leq 1. \end{aligned}$$

P_0 and T_0 are a reference pressure and temperature, respectively.

2. Pressure P and temperature T_i vary independently (two-parameter loading)

$$\begin{aligned} 0 &\leq P \leq \beta\mu_1 P_0, & 0 &\leq \mu_1 \leq 1 \\ 0 &\leq T_i \leq \beta\mu_2 T_0, & 0 &\leq \mu_2 \leq 1. \end{aligned}$$

Additionally the two cases $T_0 \leq 0$ and $T_0 \geq 0$ were studied. This corresponds to the cases $T_i \leq T_a$ and $T_i \geq T_a$, respectively. We obtain the collapse pressure by setting $T_0 = 0$.

In limit analysis the internal pressure at first yield in the symmetry plane at the inner nozzle corner A is calculated to $P_{elastic} \approx 0.048\sigma_0$. Numerical limit analysis with the basis-reduction technique leads to a collapse pressure of $2.82P_{elastic} = 0.135\sigma_0$. For comparison the limit pressure resulting from the German design rules AD-Merkblatt B9 is calculated to $P_{limit} = 2.85P_{elastic} = 0.137\sigma_0$ (see [?]).

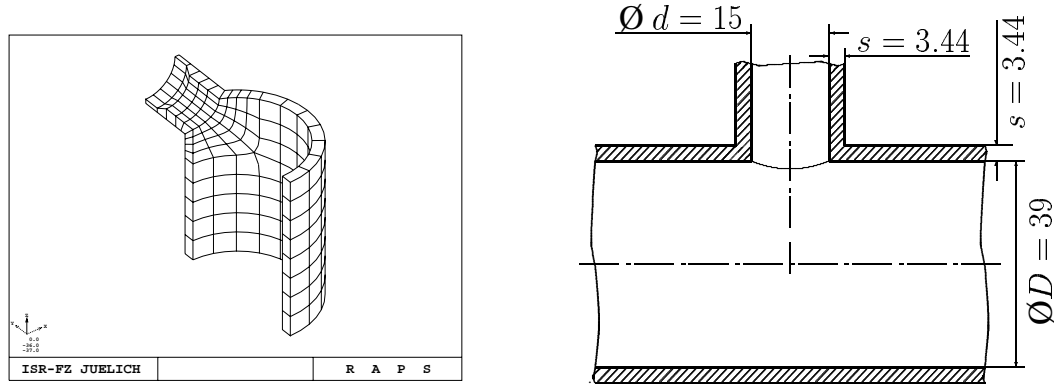


Figure 2: FE-mesh and dimension of a Pipe-Junction

From thick shell theory (see [?]) the pure elastic pressure $\hat{P}_{elastic}$ of the corresponding undisturbed pipe is

$$\hat{P}_{elastic} = \frac{(D + 2s)^2 - D^2}{\sqrt{3}(D + 2s)^2} \sigma_0 \approx 0.160\sigma_0. \quad (21)$$

The limit load factor $\hat{\beta}_{limit}$ corresponding to $\hat{P}_{elastic}$ (see [?]) is

$$\hat{\beta}_{limit} = \frac{2 \ln \left(\frac{D + 2s}{D} \right)}{1 - \left(\frac{D}{D + 2s} \right)^2} \approx 1.171. \quad (22)$$

Thus the collapse pressure \hat{P}_{limit} of the undisturbed pipe is

$$\hat{P}_{limit} = \hat{\beta}_{limit} \hat{P}_{elastic} \approx 0.188\sigma_0 \quad (23)$$

instead of $0.135\sigma_0$ for the pipe–junction. The junction presents a 28% weakening of the structure. Comparison with the elastic limit $0.0476\sigma_0$ shows, that there is a benefit of more than 181% in the ultimate load carrying capacity.

CLOUD and RODABAUGH in [?] (see also [?]) gave an upper bound on the limit pressure of a pipe–junction with

Inner pipe radius	$D = 43.815 \text{ mm}$
Inner junction radius	$d = 27.6 \text{ mm}$
Pipe thickness	$s_p = 2.54 \text{ mm}$
Junction thickness	$s_j = 1.78 \text{ mm.}$

With

$$h = \frac{d}{D} \quad \text{and} \quad g = \frac{2D}{s_p} \quad (24)$$

and the approximation formula of CLOUD and RODABAUGH the collapse pressure P_{limit} is

$$P_{limit} = \frac{\frac{3s_j^2}{2d^2} + \frac{s_p^2}{2d^2} \left(1 + \frac{2}{h\sqrt{g}}\right) + \frac{38s_j}{9gd} + \frac{s_p}{d} \left(\frac{26}{9hg} + \frac{47}{54h^2g\sqrt{g}}\right)}{\frac{38}{9g} + \frac{38}{9h^2g} + \frac{76}{27h^3g\sqrt{g}} + \frac{2}{h\sqrt{g}}} \sigma_0$$

$$\approx 0.033\sigma_0. \quad (25)$$

The elastic pressure $\hat{P}_{elastic}$ of the undisturbed pipe calculated by thick shell theory yields

$$\hat{P}_{elastic} \approx 0.062\sigma_0. \quad (26)$$

The limit load factor is $\hat{\beta}_{limit} = 1.057$ and the corresponding collapse pressure is

$$\hat{P}_{limit} \approx 0.066\sigma_0. \quad (27)$$

Thus the junction presents a 50 % weakening of the pipe. The result of the simple formula (25) ($P_{limit} = 0.033\sigma_0$) shows good agreement with the experimental results of SCHROEDER in [?] ($P_{limit} = 0.034\sigma_0$).

For the pipe–junction benchmark example ($P_{limit} = 0.134\sigma_0$) the result of equation (25) is not meaningful. Equation (25) yields $P_{limit} = 0.197\sigma_0$, but the collapse pressure of the undisturbed pipe is only $\hat{P}_{limit} = 0.160\sigma_0$. So the upper bound on the limit pressure given by the equation of CLOUD and RODABAUGH in [?] is not applicable to the benchmark example. Perhaps the greater ratio $2s/D = 0.176$ in the benchmark example instead of $2s/D = 0.058$ in SCHROEDER's experiment explains the differences.

The stresses corresponding to the thermal loading are residual stresses. So the temperature loading has no influence on the limit pressure for one– and for two–parameter

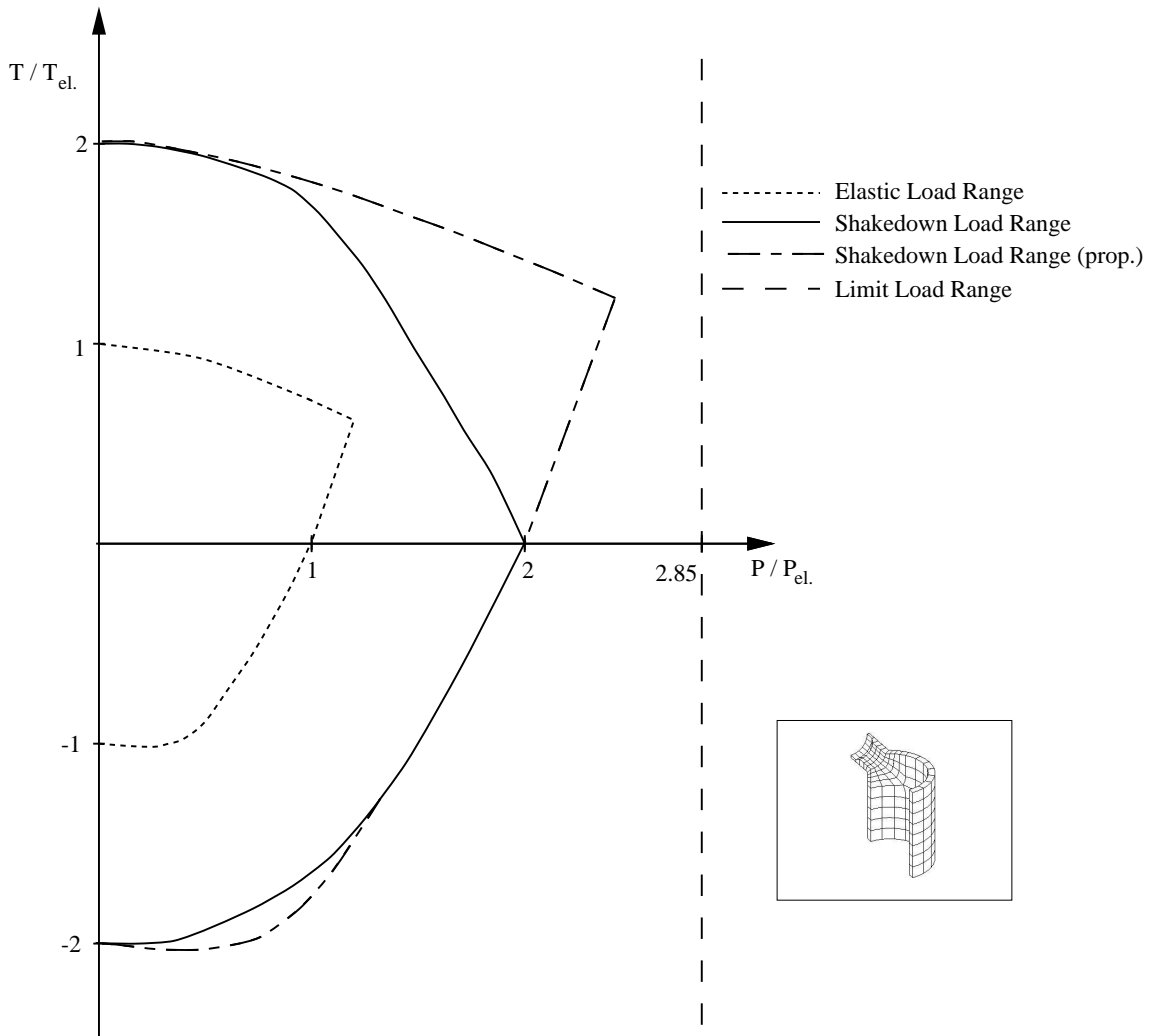


Figure 3: Interaction diagram of the pipe-junction

loading. Therefore in the interaction–diagram (see Fig. 3) of the pipe-junction the limit load range is a straight line parallel to the ordinate (the long–dashed curve). The axes of ordinates and abscissa are normed to elastic temperature–stress and to elastic pressure, respectively. The short–dashed curve in Fig. 3 marks the elastic load range in proportional loading. The kink in the line means, that for small ratio of temperature load to pressure load the presence of temperature load increase the possible pressure load to initial yielding.

The short–long–dashed curve marks the shakedown load range corresponding to the first loading condition. The shakedown factor is nearly 2 for all proportionality factors. The pipe–junction fails in every case locally at the inner nozzle point so that the factor 2 is analytical guaranteed (see the appendix for an analytic solution).

The solid curve marks the shakedown load range for two–parameter loading. The

shakedown factor varies between 1.46 and 2 related to the elastic load range.

The dimension of the residual subspace is growing during the iteration from 3 to 5. So the optimization problem has 4-6 unknowns and 2000 restrictions for one-parameter and 4000 restrictions for two-parameter loading.

The additional CPU-time for shakedown analysis is less than twice the time for the linear elastic analysis which shows, that in this case shakedown analysis is faster than limit analysis and it is much faster than computing through 10-100 inelastic load cycles until shakedown may be observed.

From an incremental calculation of the pipe-junction subjected to internal pressure we get a pressure-strain-curve (see Fig. 4). The picture shows the relation between the maximal reference strain at the inner nozzle corner A and the applied inner pressure. The axes of ordinates and of abscissa are normed to elastic pressure and strain at point A, respectively.

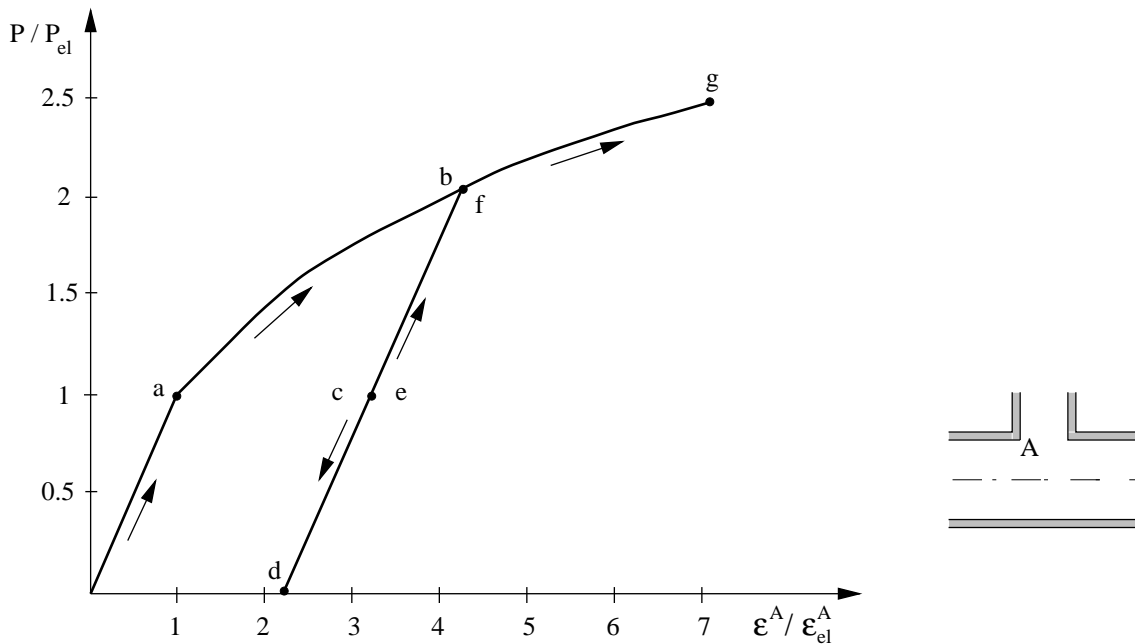


Figure 4: Pressure-strain-curve for point A of the pipe-junction

After initial elastic loading there is an increase of the loading until twice the elastic pressure is reached. Then the structure is un- and reloaded up to the previous load and above. The un- and reloading part of the curve is a line parallel to the initial elastic curve. There is no difference in the whole loading curve if there is a unloading during the loading. This means that the ultimate pressure is independent of the load-history. The remaining plastic reference strain at point A is the distance between the origin and the intersection point of the curve and the abscissa. This strain corresponds with the remaining residual stresses at point A. These normally unknown residual stresses could result from an initial loading or from the production process. However, they do not effect the ultimate pressure.

This effect corresponds to the experiments with bar-structures of MAIER-LEIBNITZ [?]. Therefore limit analysis needs no information about the load history. But it cannot predict unique strains at collapse and it must assume sufficient ductility.

Exemplary stress-distributions during the loading are shown in Fig. 5. The stresses at $P_b = 2P_{el}$ correspond to the stresses P_f after un- and reloading (see Fig. 4 for the indices).

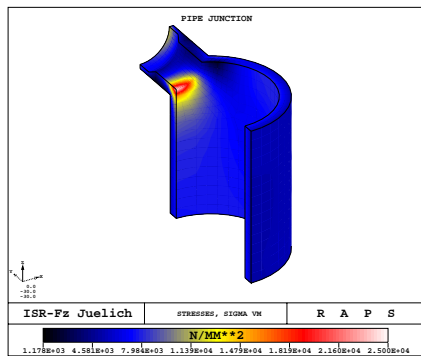
5 Summary and conclusions

Design codes for pressure vessels and piping base plastic analysis of structures under constant and varying loads on limit and shakedown analysis, respectively. These are exact theories of plasticity, which do not contain any restrictions or assumptions other than sufficient ductility of the material. Until recently their use in FEM analysis was restricted to certain types of structures and to problems of small to moderate size due to numerical problems with large-scale optimization. Therefore limit and shakedown loads were only used for stress assessment in design of passive components.

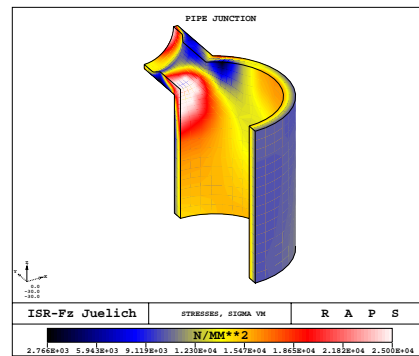
In this contribution the general purpose FEM program PERMAS was used to implement Melan's static shakedown theorem, which gives lower bounds i.e. safe loads. It was formulated as a large-scale nonlinear optimization problem. A basis-reduction method was used to obtain a sequence of smaller problems, which were solved by Sequential Quadratic Programming. Standard test problems with known solutions show that correct results are obtained at low computing times compared to incremental analyses. The solution can be made arbitrary close to the exact value since no numerical error is accumulated in load cycles. The particular implementation allows realistic FEM model sizes. The FEM based limit and shakedown analyses of a pipe junction was used as an example to compute an interaction diagram for two-parameter loading. This may be used to decide on allowable loading ranges for the junction. More complex loading may be analysed. But they cannot be represented in a similarly visual manner. The analyses may be performed at computing times and costs of only 2-10 standard elastic FEM analyses. Thus design variants may be compared and an optimum choice be made.

Limit and shakedown theorems may also provide rules and guidance for design. In the appendix we give a proof, that the shakedown factor of structures of linear kinematic hardening material subjected to proportional loading which fails locally, is equal to 2 for any hardening exponent. Therefore shakedown bounds obtained for this failure mode of structures made of perfect plastic material hold also in the presence of kinematic hardening.

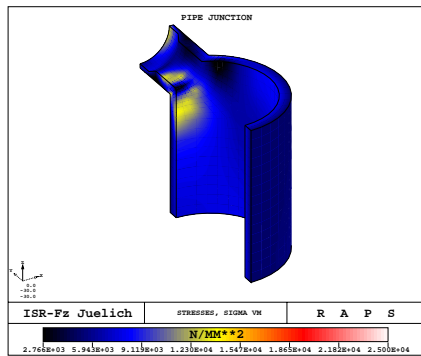
The present FEM implementation of this ongoing research is restricted to ideal plasticity with constant material coefficient. The extension to hardening material will be one of the next steps. A development towards optimum plastic design yielding the components dimensions for maximum load carrying capacity at e.g. minimum weight could be a follower of the present project.



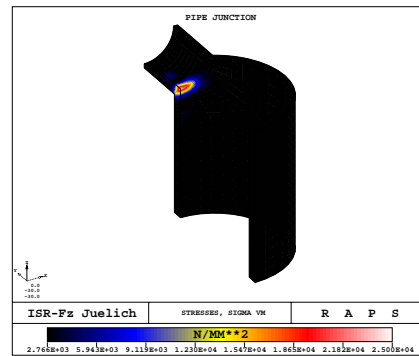
$$P_a = P_{el.}$$



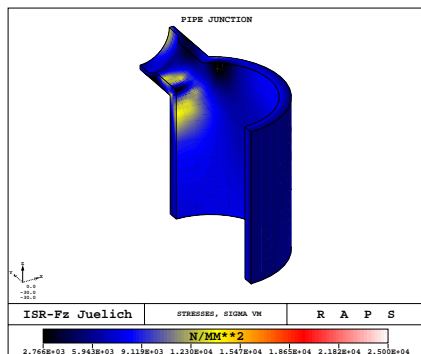
$$P_b = 2P_{el.}$$



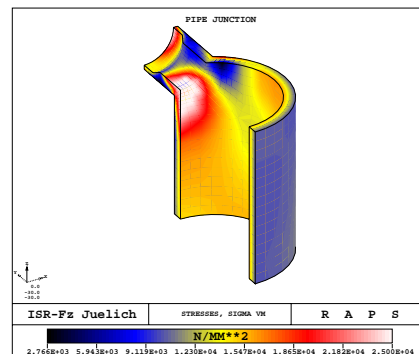
$$P_c = P_{el.}$$



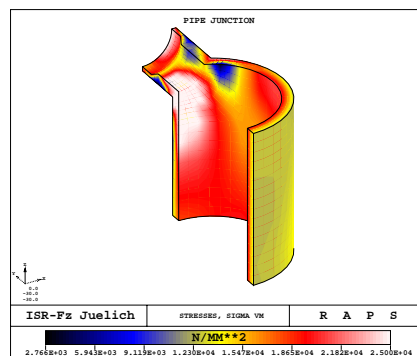
$$P_d = 0$$



$$P_e = P_{el.}$$



$$P_f = 2P_{el.}$$



$$P_g = 2.5P_{el.}$$

Figure 5: Pressure–strain–curve for point A of the pipe-junction
Staat – 14

6 Appendix

For structures made of linear kinematic hardening material the shakedown behaviour is dominated by some points of the structure, where the maximum expansion of the elastic domain is the minimum over all points $\mathbf{x} \in \Omega$:

$$\beta_{SD} = \min_{\mathbf{x} \in \Omega} (\max_{\boldsymbol{\rho}} \beta). \quad (28)$$

If only one point dominates the behaviour it is possible to solve the optimization problem analytically. In this case the shakedown load for perfectly plastic and linear kinematic hardening material correspond (see [?]). Zhang solved the problem in [?] for two-dimensional structures in two-parameter loading domain (e.g. plate with a circular hole subjected to biaxial tension) STEIN and HUANG solved the problem in principal stress space (see [?]) by the mathematical program MACSYMA. We solved the shakedown optimization problem analytically for linear kinematic hardening material in the case of local failure in one-parameter loading without the need of principal stresses. The backstresses $\boldsymbol{\alpha}$ have no restrictions in the case of linear kinematic hardening material, so that $\mathbf{y} = \boldsymbol{\rho} - \boldsymbol{\alpha}$ has no restrictions. Assuming that the maximum effective stress would appear at one point of the system, then we need to solve the optimization problem with the backstresses $\boldsymbol{\alpha}$ and

$$\min \quad -\beta \quad (29)$$

$$\text{(s.t.) } \Phi(\beta \boldsymbol{\sigma}_j^E + \mathbf{y}) \leq \sigma_0^2 \quad j = 1, \dots, NV \quad (30)$$

only in this point (see [?]). The corresponding LAGRANGE function is defined as

$$L(\beta, \mathbf{y}) = -\beta - \sum_{j=1}^{NV} \lambda_j [\sigma_0^2 - \Phi(\beta \boldsymbol{\sigma}_j^E + \mathbf{y})]. \quad (31)$$

With the abbreviation $\boldsymbol{\sigma}_j := \boldsymbol{\sigma}_j^E$ it holds

$$\Phi(\beta \boldsymbol{\sigma}_j + \mathbf{y}) = \beta^2 \boldsymbol{\sigma}_j^T \mathbf{Q} \boldsymbol{\sigma}_j + 2\beta \boldsymbol{\sigma}_j^T \mathbf{Q} \mathbf{y} + \mathbf{y}^T \mathbf{Q} \mathbf{y} \quad (32)$$

$$= (\beta, \mathbf{y})^T \underbrace{\begin{pmatrix} \boldsymbol{\sigma}_j^T \mathbf{Q} \boldsymbol{\sigma}_j & \boldsymbol{\sigma}_j^T \mathbf{Q} \\ \mathbf{Q} \boldsymbol{\sigma}_j & \mathbf{Q} \end{pmatrix}}_{=: \mathbf{A}_j} \begin{pmatrix} \beta \\ \mathbf{y} \end{pmatrix}. \quad (33)$$

In three dimensional problems the matrix $\mathbf{Q} \in \mathbb{R}^{6 \times 6}$ is defined by the von Mises function

$$\mathbf{Q} = \begin{pmatrix} 1 & -\frac{1}{2} & -\frac{1}{2} & 0 & 0 & 0 \\ -\frac{1}{2} & 1 & -\frac{1}{2} & 0 & 0 & 0 \\ -\frac{1}{2} & -\frac{1}{2} & 1 & 0 & 0 & 0 \\ 0 & 0 & 0 & 3 & 0 & 0 \\ 0 & 0 & 0 & 0 & 3 & 0 \\ 0 & 0 & 0 & 0 & 0 & 3 \end{pmatrix}. \quad (34)$$

With $\mathbf{z} := (\beta, \mathbf{y})^T$ and $\mathbf{y} \in \mathbb{R}^6$ the short form of (31) is

$$L(\mathbf{z}) = (-1, 0, \dots, 0)\mathbf{z} - \sum_{j=1}^{NV} \lambda_j [\sigma_0^2 - \mathbf{z}^T \mathbf{A}_j \mathbf{z}] \quad \text{and} \quad (35)$$

$$\nabla_{\mathbf{z}} L(\mathbf{z}) = (-1, 0, \dots, 0)^T + 2 \sum_{j=1}^{NV} \lambda_j \mathbf{A}_j \mathbf{z} \quad (36)$$

with the differential operator $\nabla_{\mathbf{z}} L(\cdot) = \left(\frac{\partial(\cdot)}{\partial \beta}, \frac{\partial(\cdot)}{\partial y_1}, \dots, \frac{\partial(\cdot)}{\partial y_6} \right)$. From the KUHN-TUCKER-conditions $\nabla_{\mathbf{z}} L(\mathbf{z}^*) = \mathbf{0}$ of a local minimum $\mathbf{z}^* = (\beta^*, \mathbf{y}^*)^T$ it follows (see [?]) with the optimal LAGRANGE multipliers λ_j^*

$$(1, \dots, 0)^T = 2 \left(\sum_{j=1}^{NV} \lambda_j^* \mathbf{A}_j \right) \mathbf{z}^* = 2 \sum_{j=1}^{NV} \lambda_j^* \left(\begin{array}{c|c} \boldsymbol{\sigma}_j^T \mathbf{Q} \boldsymbol{\sigma}_j & \boldsymbol{\sigma}_j^T \mathbf{Q} \\ \hline \mathbf{Q} \boldsymbol{\sigma}_j & \mathbf{Q} \end{array} \right) \mathbf{z}^* \quad (37)$$

$$= 2 \left(\begin{array}{c|c} \sum_{j=1}^{NV} \lambda_j^* \boldsymbol{\sigma}_j^T \mathbf{Q} \boldsymbol{\sigma}_j & \left(\sum_{j=1}^{NV} \lambda_j^* \boldsymbol{\sigma}_j \right)^T \mathbf{Q} \\ \hline \mathbf{Q} \left(\sum_{j=1}^{NV} \lambda_j^* \boldsymbol{\sigma}_j \right) & \left(\sum_{j=1}^{NV} \lambda_j^* \right) \mathbf{Q} \end{array} \right) \mathbf{z}^*. \quad (38)$$

In the local minimum \mathbf{z}^* the complementary condition of every restriction reads:

$$\lambda_j^* (\sigma_0^2 - \mathbf{z}^{*T} \mathbf{A}_j \mathbf{z}^*) = 0 \quad j = 1, \dots, NV. \quad (39)$$

After summation of all complementary conditions, we deduce with (37)

$$\sigma_0^2 \sum_{j=1}^{NV} \lambda_j^* = \sum_{j=1}^{NV} \lambda_j^* \mathbf{z}^{*T} \mathbf{A}_j \mathbf{z}^* = \mathbf{z}^{*T} \sum_{j=1}^{NV} \lambda_j^* \mathbf{A}_j \mathbf{z}^* \quad (40)$$

$$= \frac{1}{2} (1, 0, \dots, 0) \mathbf{z}^* = \frac{1}{2} \beta^*. \quad (41)$$

There is a unique representation of β^* by the LAGRANGE multipliers λ_j^* :

$$\beta^* = 2\sigma_0^2 \sum_{j=1}^{NV} \lambda_j^*. \quad (42)$$

With (42) it follows from (38)

$$\mathbf{0} = \left(\mathbf{Q} \sum_{j=1}^{NV} \lambda_j^* \boldsymbol{\sigma}_j, \sum_{j=1}^{NV} \lambda_j^* \mathbf{Q} \right) \mathbf{z}^* = \beta^* \sum_{j=1}^{NV} \lambda_j^* \mathbf{Q} \boldsymbol{\sigma}_j + \left(\sum_{j=1}^{NV} \lambda_j^* \right) \mathbf{Q} \mathbf{y}^* \quad (43)$$

$$= \beta^* \sum_{j=1}^{NV} \lambda_j^* \mathbf{Q} \boldsymbol{\sigma}_j + \frac{\beta^*}{2\sigma_0^2} \mathbf{Q} \mathbf{y}^*, \quad (44)$$

and with $\beta^* > 0$

$$\mathbf{Q} \mathbf{y}^* = -2\sigma_0^2 \sum_{j=1}^{NV} \lambda_j^* \mathbf{Q} \boldsymbol{\sigma}_j. \quad (45)$$

Now with (37) it follows

$$\frac{1}{2} = \left(\sum_{j=1}^{NV} \lambda_j^* \boldsymbol{\sigma}_j^T \mathbf{Q} \boldsymbol{\sigma}_j, \sum_{j=1}^{NV} \lambda_j^* \boldsymbol{\sigma}_j^T \mathbf{Q} \right) \mathbf{z}^* \quad (46)$$

$$= \beta^* \sum_{j=1}^{NV} \lambda_j^* \boldsymbol{\sigma}_j^T \mathbf{Q} \boldsymbol{\sigma}_j + \sum_{j=1}^{NV} \lambda_j^* \boldsymbol{\sigma}_j^T \mathbf{Q} \mathbf{y}^* \quad (47)$$

and with (45)

$$\begin{aligned} \frac{2\beta^* \sum_{j=1}^{NV} \lambda_j^* \boldsymbol{\sigma}_j^T \mathbf{Q} \boldsymbol{\sigma}_j - 1}{4\sigma_0^2} &= \left(\sum_{j=1}^{NV} \lambda_j^* \boldsymbol{\sigma}_j \right)^T \left(\sum_{j=1}^{NV} \lambda_j^* \mathbf{Q} \boldsymbol{\sigma}_j \right) \\ &= \left(\sum_{j=1}^{NV} \lambda_j^* \boldsymbol{\sigma}_j \right)^T \mathbf{Q} \left(\sum_{j=1}^{NV} \lambda_j^* \boldsymbol{\sigma}_j \right) \end{aligned} \quad (48)$$

In the case of one-parameter loading the load domain in shakedown analysis has two vertices. The corresponding fictitious elastic stresses $\boldsymbol{\sigma}_1$ and $\boldsymbol{\sigma}_2$ with $\Phi(\boldsymbol{\sigma}_1) = 0$ and $\Phi(\boldsymbol{\sigma}_2) = \sigma_0^2$ to the two load vertices read

$$\boldsymbol{\sigma}_1 = (0, 0, 0, 0, 0, 0) \text{ and } \boldsymbol{\sigma}_2 = (s_1, s_2, s_3, s_4, s_5, s_6) \quad (49)$$

From (42) follows

$$\beta^* = 2\sigma_0^2(\lambda_1^* + \lambda_2^*) \quad (50)$$

With (42) and (48) follows

$$(\lambda_1^* + \lambda_2^*)\lambda_2^* - \frac{1}{4\sigma_0^2} = \lambda_2^*\sigma_0^2 \text{ or } \lambda_1^*\lambda_2^* = \frac{1}{4\sigma_0^4}. \quad (51)$$

This means, that both restrictions must be active in the local maximum. From the KUHN-TUCKER-conditions and equations (42) and (51) follows

$$\lambda_1^* = \lambda_2^* = \frac{1}{2\sigma_0^2} \quad (52)$$

$$\beta^* = 2. \quad (53)$$

In one-parameter loading the shakedown load is twice the elastic load. This result holds independently of the hardening exponent and also for perfect plastic material [?].